Modeling of Macroscopic/Microscopic Transport and Growth Phenomena in Zeolite Crystal Solutions under Microgravity Conditions

Nikos A. Gatsonis, Andreas Alexandrou, Hui Shi, Bernard Ongewe
Mechanical Engineering Department
100 Institute Rd.
Worcester Polytechnic Institute, Worcester MA 02139
Phone: (508)-831-5576, 831-5147
e-mail: gatsonis@wpi.edu, andalexa@wpi.edu

Albert Sacco, Jr.
Chemical Engineering Department
242 Snell Engineering Center
Northeastern University, Boston, MA 02115
Phone: (617)-373-7910
e-mail: asacco@coe.neu.edu

Introduction

Crystals grown from liquid solutions have important industrial applications. Zeolites, for instance, a class of crystalline aluminosilicate materials, form the backbone of the chemical process industry worldwide, as they are used as adsorbents and catalysts [Meier, 1986; Barrer, 1986]. Many of the phenomena associated with crystal growth processes are not well understood due to complex microscopic and macroscopic interactions. Microgravity could help elucidate these phenomena and allow the control of defect locations, concentration, as well as size of crystals. Microgravity in an orbiting spacecraft could help isolate the possible effects of natural convection (which affects defect formation) and minimize sedimentation. In addition, crystals will stay essentially suspended in the nutrient pool under a diffusion-limited growth condition. This is expected to promote larger crystals by allowing a longer residence time in a high-concentration nutrient field. Among other factors, the crystal size distribution depends on the nucleation rate and crystallization. These two are also related to the "gel" polymerization/depolymerization rate. Macroscopic bulk mass and flow transport and specially gravity, force the crystals down to the bottom of the reactor, thus forming a sedimentation layer. In this layer, the growth rate of the crystals slows down as crystals compete for a limited amount of nutrients. The macroscopic transport phenomena under certain conditions can, however, enhance the nutrient supply and therefore, accelerate crystal growth.

Several zeolite experiments have been performed in space with mixed results. The results from our laboratory have indicated an enhancement in size of 30 to 70 percent compared to the best ground based controls, and a reduction of lattice defects in many of the space grown crystals [Sand et al., 1987; Sacco et al., 1993]. Such experiments are difficult to interpret, and cannot be easily used to derive empirical or other laws since many physical parameters are simultaneously involved in the process. At the same time, however, there is increased urgency to develop such an understanding in order to more accurately quantify the process.

In order to better understand the results obtained from our prior space experiments, and design future experiments, a detailed fluid dynamic model simulating the crystal growth mechanism is required. This will not only add to the fundamental knowledge on the crystallization of zeolites, but also be useful in predicting the limits of size and growth of these important industrial materials. Our objective is to develop macro/microscopic theoretical and computational models to study the effect of transport phenomena in the growth of crystals grown in solutions. Our effort has concentrated so far in the development of separate macroscopic and microscopic models. The major highlights of our accomplishments are described bellow.

Macroscopic Model

The crystal growth process is modeled as a multiphase (solid and fluid phases) system. The macroscopic fluid dynamics model accounts for the continuous solid and fluid phases. Throughout the process there is continuous interaction between the two phases. For the time being, the crystal growth process is modeled by an exponential law, expressed as $\dot{r} = \alpha e^{-\beta t}$, where α and β depend on microscopic fluid and chemical interactions. In the future, this model will be combined with a microscopic model based on a Monte-Carlo approach. Following [Druzhinin, 1995], the mass and momentum equations are formulated as follows.

Solid Phase
The continuity equation is

$$\frac{\partial s}{\partial t} + \nabla \cdot (s\boldsymbol{u}_s) = \dot{r}_s \tag{1}$$

where s is solid volume fraction, $\boldsymbol{u}_s$ is solid velocity vector, $\dot{r}_s$ is rate of crystal growth divided by the density of the solid ρ_s. i.e., $\dot{r}_s = \dot{r} / \rho_s$.

The momentum equation is

$$\frac{\partial(s\boldsymbol{u}_{s_i})}{\partial t} + \nabla \cdot (s\boldsymbol{u}_{s_i}\boldsymbol{u}_s) = sF_i + sg_i, \qquad i = 1,2,3. \tag{2}$$

where F_i is the interaction force between the two phases, and, g_i the gravity acceleration component each along the coordinate direction, x_i.

Fluid Phase
The continuity equation is

$$\frac{\partial(1-s)}{\partial t} + \nabla \cdot ((1-s)\boldsymbol{u}_f) = -\dot{r}_f \tag{3}$$

where $\boldsymbol{u}_f$ is the fluid velocity vector and $\dot{r}_f$ the fluid depletion rate divided by the density of the fluid, i.e., $\dot{r}_f = \dot{r} / \rho_f$. Notice that $\dot{r}_s \rho_s = \dot{r}_f \rho_f$. The negative sign in $\dot{r}_f$ shows that fluid is depleted by supplying nutrients for the crystal growth.
The momentum equation is

$$\frac{\partial((1-s)\boldsymbol{u}_{f_i})}{\partial t} + \nabla \cdot ((1-s)\boldsymbol{u}_{f_i}\boldsymbol{u}_f) = -(\nabla p)_i - s\delta F_i + (1-s)g_i + (\nabla \cdot \hat{\tau})_i, i = 1,2,3. \tag{4}$$

where δ is the density ratio ρ_s/ρ_f. p is the fluid pressure divided by ρ_f. The two phases are coupled through the interaction force F_i. In our model, ρ_s and ρ_f are assumed to be constant. $\hat{\tau}$ is the viscous stress tensor divided by the density of the fluid defined for the incompressible Newtonian fluid phase as:

$$\hat{\tau}_{ij} = (1-s)\nu\left(\frac{\partial u_{f_i}}{\partial x_j} + \frac{\partial u_{f_j}}{\partial x_i}\right) \qquad i,j = 1,2,3. \tag{4a}$$

In the above expression ν is the kinematic viscosity of the fluid phase.

Constitutive Relations

In the case of small heavy particles, the major contribution to the interaction force is from the viscous drag force [Maxey and Riley, 1983]. For particles with Reynolds number of order of unity, the viscous drag force is expressed by the following empirical formula:

$$F_i = \frac{1}{\tau_p}\left(u_{f_i} - u_{s_i}\right)f\left(Re_p\right) \tag{5}$$

Where $\tau_p = \dfrac{d^2\delta}{18\nu}$, $Re_p = \dfrac{|u_f - u_s|}{\nu}d$, and $f\left(Re_p\right) = 1 + 0.15\,Re_p^{2/3}$.

The following relations are used to describe the growth rate

$$\dot{r}_s = \frac{\alpha}{\rho_s}e^{-\beta t} = \alpha_s e^{-\beta t} \quad \dot{r}_f = \frac{\alpha}{\rho_f}e^{-\beta t} = \alpha_f e^{-\beta t} \tag{6}$$

Boundary and Initial Conditions

On the interior surface of the reactor, a no-slip boundary condition ($u_f = 0$) for the fluid phase and a slip boundary condition ($u_s \cdot n = 0$) for crystal particle phase is imposed, here n is the unit normal vector on the surface. Initially, both phases are assumed to be stationary. The particle phase is initialized by a specified solid volume fraction distribution in the reactor. The subsequent motion of the interactive phases is induced by gravity.

Results and Discussions

Fig. 1(a) shows the solid velocity field at an intermediate time in the settling process of particles. As a result of the gravity, the particles settle to the bottom and collect around the center due to the action of fluid flow. Fig. 1(b) shows the fluid velocity field whose main feature is the recirculation region consisting of two large vortices. Fig. 1(c) represents the fluid pressure contour showing that the initial linear static pressure distribution changes mainly in the particle region. Fig. 1(d) illustrates the evolution of solid volume fraction along the centerline of the container: as time progresses, the particles shift to the bottom being slightly diffused. The maximum value decreases with time. Fig. 2. represents the effect of variable gravity levels: the larger the gravity level, the faster the particles settle. Fig. 3 shows the particle sedimentation on the bottom of the reactor: with larger gravity level, the particles settle faster.

Microscopic Model

The model is based on the Direct Simulation Monte Carlo (DSMC) method and is aimed at capturing the effects of macroscopic flow on the growth and size distribution of the growing

crystals. The system include nutrients, crystals and the mean motion of the fluid in a domain that models realistic systems. The grid is based on the mean-free path (λ_{nn}) of collisions between nutrients. The length of this grid may be modified to include collisional interactions between nutrients and the fluid phase of the solution. Nutrients and crystals move and collide under the actin of gravity and fluid-drag forces.

Nucleation Process

In a zeolite solution nucleation and crystallization overlap and interact with each other. These processes have been modeled in a variety of methods [Thompson and Dryer, 1985]. The nucleation will be introduced with a Monte Carlo model that resembles closely the actual process. The nucleation sites will be created in random with a probability based on a model that describes the nucleation as a function of local thermodynamic. Another alternative is to introduce nucleation via a chemically reacting process based on a rate coefficient that depends on thermodynamic parameters. Ultimately, this issue will be resolved using experimental data.

Collisions between Nutrients

Elastic collisions between nutrients are modeled via the No-Time-Counter (NTC) method [Bird, 1994]. Collisional pairs are selected in cells and the collision probability in each computational cell is calculated based on the NTC method. The model employs the hard sphere (VHS) in evaluating collision cross sections.

Nutrient Impingement and Crystal Growth Process

The nucleation sites grow to crystals of finite size. Particle methods are ideal to model the crystallization process as well. The level of modeling however, is dictated by the computational requirements. Our approach is to describe the key physical processes with a model that will be refined through successive iterations with data comparisons. For this reason, we initially concentrate our efforts in the determination of the size distribution of the crystals.

The crystals are considered as spherical particles that grow after their attraction and attachment of nutrients. Within the framework of the DSMC, an attachment probability P_a will be evaluated in those cells in which nucleation sites or crystals exist. This probability will be calculated on concentrations or surface kinetics based on impingement rates.

Particle Weighting Scheme

Given that the crystal particles in our simulations are real particles, different particle weights have to be assigned to the crystal and nutrient 'species' respectively. The primary concern in enacting this scheme is the treatment of collisions between simulation particles that are represented by different particle weights. In this event, linear momentum and energy are not conserved by the conventional NTC elastic collision model. This is accomplished in our model using a conservative multi-weight method.

Results and Discussion

Preliminary simulations were performed in order to test the motion and collision algorithms of the code. The simulations compared the effects of gravity on settling time of crystals in the absence of fluid/particle drag. The domain is initialized with 912 spherical crystal particles in a cubic container with size 0.3 m. The spherical crystals have a diameter of 4.17×10^{-6} m, and mass
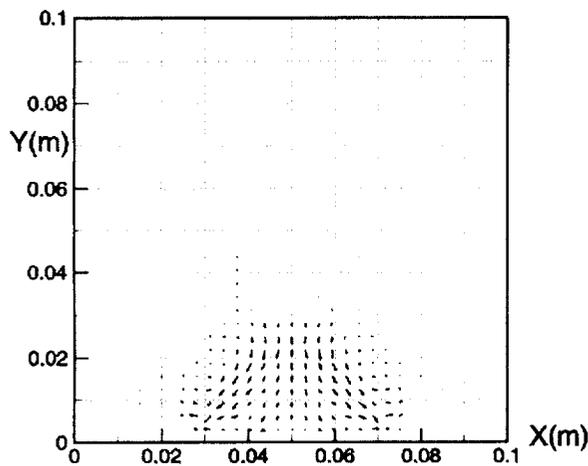
of 6.63×10^{-14} kg. Results are shown in Figures 4 and 5 for 1-g and 0-g conditions respectively at 0.6 seconds after initialization. At this point, the center of gravity of the crystal particles was calculated to be at a height of 0.09 m and 0.073 m respectively for the 0-g and 1-g cases. As shown, the imposition of a gravitational force field has immediate effects on particle distribution. Future simulations will determine the extent to which this distribution gradient affects the growth rate and subsequent final size of the crystals as they compete for nutrients.

Acknowledgments

References

1. W.M. Meier, "Zeolites and Zeolite-like Materials", New Developments in Zeolite Science and Technology, Proceeding of the 7th international Zeolite Conference, Tokyo, Aug., 1986.
2. R.M. Barrer, "Porous Crystals: A Perspective", New Developments in Zeolite Science and Technology, Proceeding of the 7th international Zeolite Conference, Tokyo, August, 1986.
3. Sacco, Jr., R.W. Thompson, and A.G. Dixon, ``Zeolite Crystal Growth in Space- What has been learned," AIAA 93-0473.
4. Sand, L. B., Sacco, A., Thompson, R. W., and Dixon, A. G.,``Large Zeolite Crystals: their potential growth in space", Zeolites, Vol.7, pp387-392, 1987.
5. Maxey, M.R., and James J. Riley, ``Equation of Motion for a small rigid sphere in a nonuniform flow", *Phys. Fluids 26(4)*, 1983
6. Druzhinin, O.A., "On the two-way interaction in two-dimensional particle-laden flows:the accumulation of particles and flow modification", *J. Fluid Mech., Vol. 297, pp 49-76*, 1995
7. Thompson R.W. and A. Dryer, *Zeolites*, Vol. 5, 202 , 1985.
8. Bird, G., Molecular gas dynamics and the direct simulation of flows, Oxford, 1994.

(a) Particle flux: ref. value: 0.01 m·s⁻¹ →
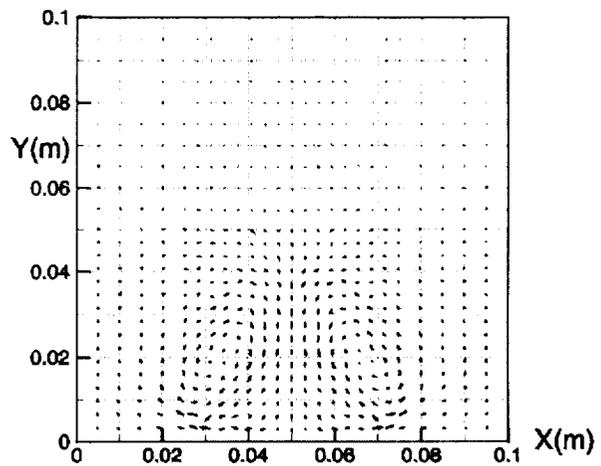
(b) Fluid flux: ref. value: 0.1 m·s⁻¹ ·

(c) Pressure contour

(d) Evolution of solid volume fraction along the centerline.
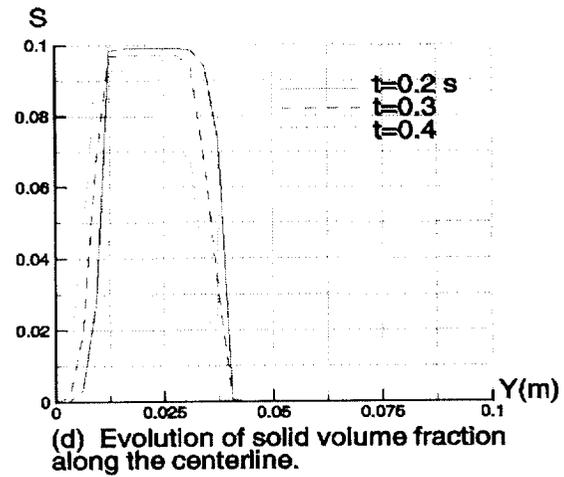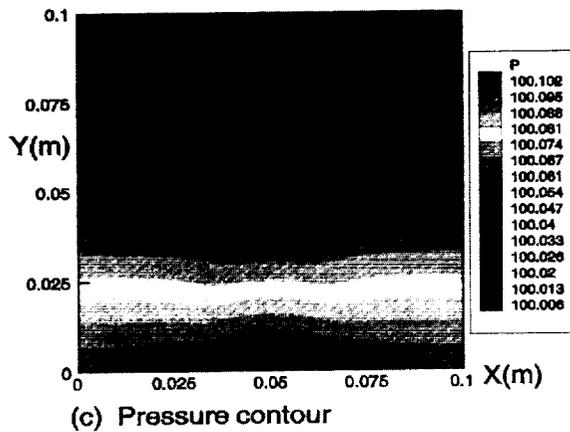
Fig. 1 Results at time 0.37 s. for a 2-D reactor. $v = 10^{-5}$ m^2·s^{-1}. $a = 1.0$ m·s^{-2}. $d = 10^{-4}$ m.

Fig. 2 Settling distance of mass center of particles versus time for variable gravities, $v = 10^{-5}$ m^2·s^{-1}, $d = 10^{-4}$ m.

Fig. 3 Particle sedimentation on the bottom for $v = 10^{-5}$ m^2·s^{-1}, $d = 10^{-4}$ m.
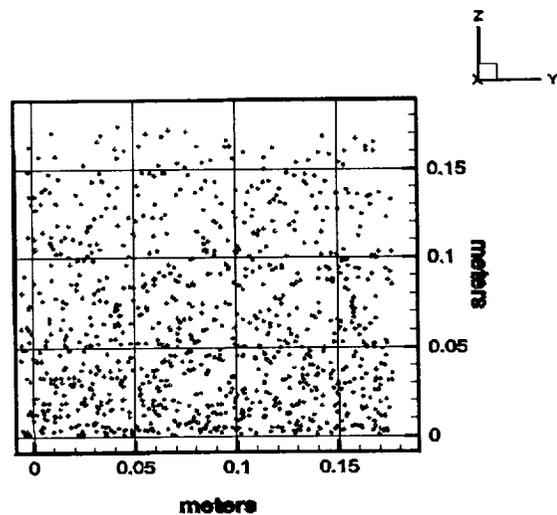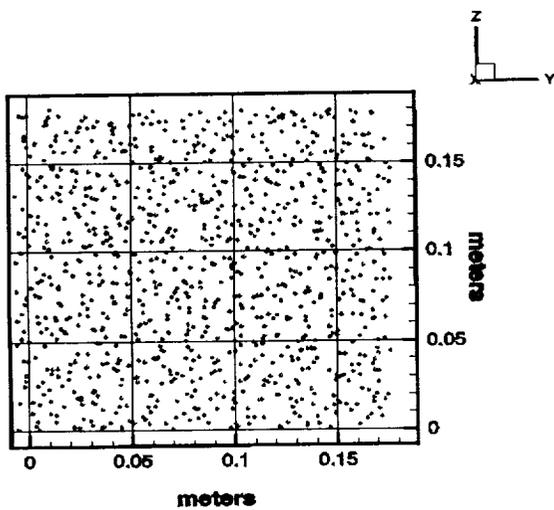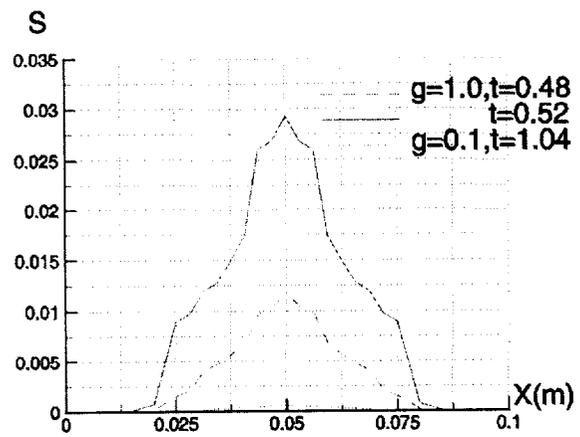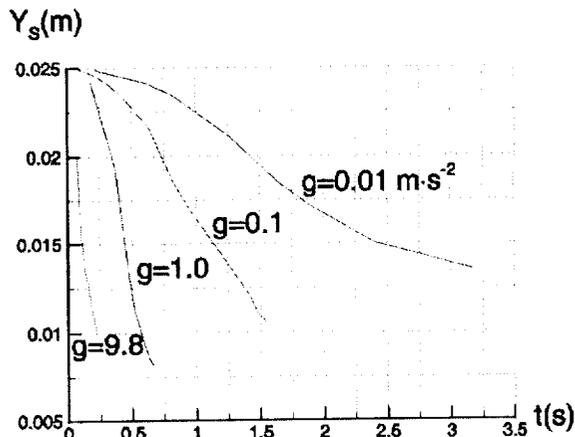

Fig. 4: Crystal particle distribution after 0.6 Seconds (0-g)

Fig. 5: Crystal particle distribution after 0.6 seconds (1-g)

574